1 **Loss of NR5A1 in Sertoli cells after sex determination changes their**

2 **cellular identity and induces their death by anoikis**

3 Sirine SOUALI-CRESPO[1], Diana CONDREA[1], Nadège VERNET[1], Betty FÉRET[1],

4 Muriel KLOPFENSTEIN[1], Erwan GRANDGIRARD[1,3], Violaine ALUNNI[1,2], Marie

5 CERCIAT[1,3], Matthieu JUNG[1,3], Chloé MAYERE[4], Serge NEF[4], Manuel MARK[1,5],

6 Frédéric CHALMEL[6*], and Norbert B. GHYSELINCK[1*#]

7 1. Institut de Génétique et de Biologie Moléculaire et Cellulaire (IGBMC),

8   Département de Génétique Fonctionnelle et Cancer, Centre National de la

9   Recherche Scientifique (CNRS UMR7104), Institut National de la Santé et de la

10   Recherche Médicale (INSERM U1258), Université de Strasbourg (UNISTRA),

11   1 rue Laurent Fries, BP-10142, F-67404 Illkirch Cedex, France

12 2. GenomEast Platform, France Génomique consortium, IGBMC, 1 rue Laurent

13   Fries, F-67404 Illkirch Cedex, France

14 3. Imaging Center, IGBMC, F-67404 Illkirch Cedex, France

15 4. Department of Genetic Medicine and Development, Faculty of Medicine,

16   University of Geneva, Geneva, Switzerland

17 5. Service de Biologie de la Reproduction, Hôpitaux Universitaires de Strasbourg

18   (HUS), France

19 6. Univ Rennes, EHESP, Inserm, Irset (Institut de recherche en santé,

20   environnement et travail) - UMR_S 1085, F-35000 Rennes, France

21 * These authors contributed equally to this work

22 # Author for correspondence: norbert@igbmc.fr

23 Tel: +33 388 655 674; Fax: +33 388 653 201

24 **Keywords:** anoikis, cell-death, fetal gonad, integrin, Leydig, testis, SF-1, single-cell.

26 **ABSTRACT**

27   **NR5A1 is an orphan nuclear receptor crucial for gonadal development in**

28 **mammals. In the mouse testis it is expressed both in Sertoli cells (SC) and**

29 **Leydig cells (LC). To investigate its role posteriorly to sex determination, we**

30 **have generated and analysed mice lacking NR5A1 in SC from embryonic day**

31 **(E) 13.5 onwards (*Nr5a1*SC–/– mutants). Ablation of *Nr5a1* impairs the expression**

32 **of genes characteristic of SC identity (e.g., *Sox9*, *Amh*), makes SC to**

33 **progressively die from E14.5 by a *Trp53*-independent mechanism, and induces**

34 **disorganization of the testis cords, which, together, yields germ cells (GC) to**

35 **prematurely enter meiosis and die, instead of becoming quiescent. Single-cell**

36 **RNA-sequencing experiments revealed that *Nr5a1*-deficient SC acquire a pre-**

37 **granulosa cell-like identity, and profoundly modify the landscape of the**

38 **adhesion molecules and extracellular matrix they express. We propose**

39 **therefore that SC lacking NR5A1 transdifferentiate and die by anoikis. Fetal LC**

40 **do not display major changes in their transcriptome, indicating that SC are not**

41 **required beyond E14.5 for their emergence or maintenance. In contrast, adult**

42 **LC were missing in *Nr5a1*SC–/– postnatal testes. In addition, adult males display**

43 **Müllerian duct derivatives (i.e., uterus, vagina), as well as a decreased**

44 **anogenital distance and a shorter penis that can be explained by loss of AMH**

45 **production and defective HSD17B1- and HSD17B3-mediated synthesis of**

46 **testosterone in SC during fetal life. Together, our findings indicate that *Nr5a1***

47 **expressed in SC after the period of sex determination safeguards SC identity,**

48 **which maintains proper seminiferous cord organization and prevents GC to**

49 **enter meiosis.**

50   **INTRODUCTION**

51   Testis and ovary both originate from a bipotential gonad, which is composed of

52   somatic progenitor cells that are competent to adopt one or the other sex-specific cell

53   fate, and of primordial germ cells (GC). Sex determination initiates at around

54   embryonic day (E) 11.5, from when somatic progenitor cells undergo sex-specific cell

55   differentiation. The specification of the supporting cell lineage [i.e., either Sertoli cells

56   (SC) in the testis upon SRY expression, or pre-granulosa cells (pGrC) in the ovary

57   upon WNT/CTNNB1 signalling stabilization] is the first essential step in this process.

58   Following supporting cell differentiation, the sex-specific fate decision propagates to

59   the GC and to other somatic lineages, including the steroidogenic cells Leydig cells

60   (LC) in the testis, which, in turn, drive acquisition of primary and secondary sexual

61   characters at later stages of development, through hormone secretion [1-3]. In

62   humans, mutations in genes driving this complex developmental process can give

63   rise to a group of defects known as disorders of sex development (DSD), the

64   diagnosis and the management of which requires an understanding of the molecular

65   mechanisms underpinning cell differentiation [4].

66   Amongst the genes responsible for DSD is *Nr5a1*, encoding the orphan nuclear

67   receptor NR5A1 [5], a transcription factor expressed at early stages of development,

68   when cells are partitioned into adrenal and gonadal primordium [6]. NR5A1 controls

69   the expression of genes implicated in proliferation, survival and differentiation of

70   somatic progenitor cells [7]. Therefore, knock-out of *Nr5a1* in the mouse results in

71   regression of the gonads by E11.5 due to apoptosis of somatic cells, and agenesis of

72   the adrenal gland [8]. From E11.5, NR5A1 and SRY are expressed in the bipotential

73   supporting cells of male embryos, where they upregulate SOX9 expression, initiating

74   thereby pre-SC and ultimately SC differentiation [2,3,9]. Once specified, the SC start

75   forming cords by enclosing GC as early as E12.5 in the mouse [10], providing them

76   with a specialized environment that promotes their survival and orchestrates their

77   differentiation [11]. SC also (i) allow the differentiation of fetal LC (FLC) through

78   paracrine Desert Hedgehog (DHH) signalling [12], (ii) produce, under the control of

79   NR5A1 and SOX9, high levels of anti-Müllerian hormone (AMH), which triggers the

80   regression of the Müllerian duct normally giving rise to the female genitalia [13].

81   Because gonads are absent in *Nr5a1*-null mice [8], studying the cell-specific

82   roles of NR5A1 in the developing testis required analysis of mice bearing tissue-

83   targeted mutations. Here we have analysed the outcome of *Nr5a1* ablation in SC

84   from E13.5 onwards. We show that loss of NR5A1 from this stage induces some SC

85   to transdifferentiate into female somatic cells, and to die by a *Trp53*-independent

86   mechanism related to anoikis.

87   **RESULTS**

88   ***Deletion of* Nr5a1 *in Sertoli cells***

89   To achieve *Nr5a1* ablation in SC after sex determination, we introduced the

90   *Plekha5*$^{Tg(AMH-cre)1Flor}$ transgene [14] in mice bearing *lox*P-flanked alleles of *Nr5a1* and

91   a Cre-dependent reporter transgene [15]. Cre-mediated recombination was assessed

92   by immunohistochemistry (IHC) using antibodies recognizing the yellow fluorescent

93   protein (YFP). Surprisingly, YFP was detected in all SC of embryonic day (E) 12.5

94   gonads (arrows, **Fig.1A,B**), indicating Cre-mediated excision occurred earlier than

95   anticipated [14]. However, the NR5A1 protein was still detected in SC at E12.5

96   (**Fig.1A,B**). At E13.5, the nuclei of SC were all NR5A1-positive in the control

97   (**Fig.1C**), but NR5A1-negative in the mutant testis (**Fig.1D**). Importantly, NR5A1 was

98   still detected in the nuclei of LC, identified by their expression of the steroid 3 beta-

99   hydroxy-steroid dehydrogenase type 1 (HSD3B1), in both control and mutant testes

100 (**Fig.1E,F**). Thus, NR5A1 was lost selectively in SC from E13.5 onwards, generating

101 males hereafter called *Nr5a1*$^{SC-/-}$ mutants.

Ablation of Nr5a1 *in SC impairs expression of SOX9, SOX8, SOX10 and AMH*

103 As NR5A1 regulates the expression of *Amh* and *Sox9* genes [9,16], we tested

104 expression of these two proteins by IHC. Both AMH and SOX9 were detected at

105 normal levels at E12.5 (**Fig.2A,B,G,H**). Their expression decreased progressively

106 between E13.5 and E14.5 in *Nr5a1*$^{SC-/-}$ mutant testes (**Fig.2C-F,I-L**). At E14.5, only

107 few *Nr5a1*-deficient SC were SOX9-positive, some of which with cytoplasmic SOX9

108 (compare insets, **Fig.2K,L**). The expression of SOX8 and SOX10 was also

109 decreased in *Nr5a1*$^{SC-/-}$gonads (**Suppl.Fig.1**). Accordingly, the steady state levels of

110 *Amh*, *Sox9* and *Sox8* mRNAs was decreased in *Nr5a1*$^{SC-/-}$ whole gonads (**Fig.2S**).

111 The level of prostaglandin D2 synthase (*Ptgds*) mRNA, another SOX9 target-gene

112 [17], was also reduced in E14.5 *Nr5a1*$^{SC-/-}$ testes. This finding may explain the

113 cytoplasmic localization of SOX9 in some SC since prostaglandin D2, the end

114 product of PTGDS, is required for SOX9 nuclear translocation [18].

115 In parallel, we analysed the expression of GATA4 and WT1, important for *Amh*

116 expression and SC differentiation, respectively [19,20]. Both were detected at similar

117 levels in SC nuclei of control and mutant testes, from E12.5 to E14.5 (**Fig.2M-R;**

118 **Suppl.Fig.1**).

Nr5a1*-deficient SC die through a TRP53-independent mechanism*

120 Thanks to the expression of the YFP-reporter we quantified the surface

121 occupied by SC (green pixels) relative to the whole testis surface (**Fig.3A,D**). At

122 E14.5, this ratio was about 30% lower in mutant than in control testes [28.3 ± 3.8

123 (n=5) versus 37.9 ± 2.5 (n=5), respectively; p<0.01]. This suggested that *Nr5a1*-

124   deficient SC had either shut down expression of YFP or had disappeared from the

125   testis. If YPF expression was shut down, the excised *Nr5a1* allele (L-) should be

126   present in the testis at birth. If SC were lost, it should no longer be detected. PCR

127   analysis of genomic DNA showed that the L– allele was not amplified in *Nr5a1*$^{SC-/-}$

128   mutants (**Suppl.Fig.2A**), indicating that *Nr5a1*-deficient SC were lost from the mutant

129   testis. In agreement with this possibility, numerous cells displaying features of SC

130   (i.e., located at the periphery of the testis cords, amongst GATA4-expressing SC)

131   were TUNEL-positive in E14.5 *Nr5a1*$^{SC-/-}$ testis (arrowheads, **Fig.3E,F**). This

132   indicates that NR5A1-deficient SC progressively died.

133   Because TRP53 was not detected in fetal SC at E14.5 (**Fig.3G,H**), we

134   wondered whether it was functionally involved in SC-death. We introduced

135   conditional alleles of *Trp53* [21] in *Nr5a1*$^{SC-/-}$ mutants bearing the YFP reporter

136   transgene. Efficient ablation of *Trp53* was assessed by PCR on genomic DNA

137   extracted form FACS-purified, YFP-positive, SC (**Suppl.Fig.2B**). E14.5 *Nr5a1*$^{SC-/-}$

138   and *Nr5a1*$^{SC-/-}$;*Trp53*$^{SC-/-}$ mutants displayed similar reduced surfaces occupied by

139   SC (**Fig.3I,J**, compare with 3A), out of which most of them had lost expression of

140   SOX9. At post-natal day 15 (PND15), both *Nr5a1*$^{SC-/-}$ and *Nr5a1*$^{SC-/-}$;*Trp53*$^{SC-/-}$

141   testes lacked SC-surrounded seminiferous tubules, but contained interstitial cells, out

142   of which about half of them were HSD3B1-positive LC (**Fig.3K-P**). At adulthood, none

143   of the interstitial cells expressed the adult LC-specific marker BHMT [22], indicating

144   this cell-type was unable to emerge (**Fig.3Q-S**). Altogether, this indicates that

145   NR5A1-deficient SC died, even though they lacked TRP53, yielding a postnatal testis

146   made of FLC and other interstitial cells.

147   **Nr5a1$^{SC-/-}$ adult males exhibit Müllerian duct retention**

148   To analyse the outcome of the loss of SC and AMH production in *Nr5a1*^{SC−/−}

149   mutants, the male phenotype was investigated at PND60. They all were sterile and

150   had a shorter anogenital distance (AGD) index [0.30 ± 0.03 mm/g of body weight

151   (n=16), versus 0.36 ± 0.02 mm/g (n=17) in controls; p<0.001] (**Fig.4A,C**). At autopsy

152   (n = 8), they displayed normal derivatives of the Wolffian ducts (i.e., epididymis, vas

153   deferent, seminal vesicle, ampullary glands) and the urogenital sinus (i.e., prostatic

154   lobes) (**Fig.4E,F**). However, they also displayed Müllerian duct derivatives (**Fig.4F-**

155   **H**), namely a vagina, an uterine body and bilateral, uterine horns, which were either

156   incomplete and truncated (6 out of 8), or complete on one side (2 out of 8).

157   Histological analyses revealed that the uterine body and vagina displayed a columnar

158   epithelium (**Fig.4I**) and a stratified, squamous epithelium (**Fig.4J**), as anticipated for

159   these female organs.

160   Nonetheless, *Nr5a1*^{SC−/−} males displayed 40% lighter seminal vesicles

161   [4.71 ± 1.66 mg/g of body weight (n=17) versus 7.43 ± 1.22 mg/g (n=16) in controls;

162   p<0.05] and 10% shorter penis bones [6.7 ± 0.4 mm (n=17) versus 7.5 ± 0.3 mm

163   (n=16) in controls; p<0.05] (**Fig.4B,D**). As AGD, seminal vesicle growth and penis

164   bone length vary as a function of androgen exposure [23], we tested blood

165   testosterone levels. They were comparable at birth [0.25 ± 0.17 ng/ml (n=10) in

166   mutants, versus 0.22 ± 0.10 ng/ml serum (n=10) in controls; p=0.59], and at PND60

167   [0.38 ± 0.17 ng/ml (n=17) in controls, versus 0.43 ± 0.23 ng/ml serum (n=16) in

168   controls; p=0.68], indicating normal testosterone production.

169   ***Transcriptomic signatures of cells in control and* Nr5a1 *-deficient gonads.***

170   We then performed single-cell RNA sequencing (scRNA-seq) experiments

171   using dissociated cell suspensions obtained from 12 control and 16 *Nr5a1*^{SC−/−} whole

172   testes at E14.5. After data processing and quality control, we assembled an atlas

173   composed of 3,988 and 5,010 control and mutant testicular cells, respectively. On

174   average, we detected ~13,860 unique molecular indices (UMIs) and ~3,556 genes in

175   each individual cell. The 8,998 testicular cells were partitioned into 23 cell clusters

176   (termed C1-C23) and projected into a two-dimensional space (**Fig.5A; Table.S1**).

177   Known marker genes of distinct cell-types were used to identify each cluster

178   (**Suppl.Fig.3**).

179   Only a few changes of gene expression were observed between control and

180   *Nr5a1$^{SC-/-}$* testes for endothelial, immune and perivascular cells. In Leydig, interstitial,

181   and coelomic epithelium cells the expression of 59, 49, and 47 genes was

182   deregulated (**Table.S2**). Functional analysis revealed that down-regulated genes

183   were related to ribosome in Leydig (14 genes, *p* value<4.8^{e-15}) and interstitial cells

184   (12 genes, *p* value<1.3^{e-10}) (**Suppl.Fig.4; Table.S3**). In GC, the expression of 636

185   genes was significantly deregulated (**Table.S1**), amongst which *Stra8* and *Rec8* were

186   up, while *Nanos2* and *Piwil4* were down (**Fig.5B**). Processes such as DNA

187   recombination (33 genes, *p* value<2.0^{e-10}), meiotic cell cycle (32 genes, *p* value<1.1^{e-9})

188   and oocyte differentiation (8 genes, *p* value<5.6^{e-3}) were identified amongst the

189   upregulated genes (**Suppl.Fig.4; Table.S3**). In agreement with this finding we

190   showed that GC were in the S-phase of the meiotic prophase at E14.5 and E15.5 in

191   *Nr5a1$^{SC-/-}$* testes instead of becoming mitotically quiescent, as in the control

192   situation. Accordingly, many GC of the *Nr5a1$^{SC-/-}$* testes expressed meiotic proteins,

193   such as STRA8 or REC8, and died because of premature meiotic initiation

194   (**Suppl.Fig.5**).

195   Three clusters of SC were identified (C18, C19 and C21), out of which C19 and

196   C21 were mainly composed of control and NR5A1-deficient SC, respectively

197   (**Fig.5A**). Almost all SC of C18 were mitotic (**Suppl.Fig.3**). In total, 1,671 genes were

198 significantly deregulated in SC (**Suppl.Table.S1**), amongst which *Amh*, *Sox9* and

199 *Ptgds* were down as anticipated (see above), while *Wnt4*, *Fst* and *Rspo1* were up

200 (**Fig.5C**). We confirmed deregulated expression of some by IHC (**Fig.5D-K**) and that

201 of others by RT-qPCR (**Fig.5L**), validating thereby the scRNA-seq experiment.

202 According to its transcriptomic signature, cluster C20 was assigned the *rete*

203 *testis* identity (**Suppl.Fig.3)**. This structure is a set of ducts, through which

204 spermatozoa are transported from the gonad via the efferent duct to the epididymis

205 [24]. At E14.5, the *rete testis* is identified as epithelial cords between the

206 mesonephric tubules and the testis cords (**Suppl.Fig.6A**). The *rete testis* cells

207 express *Nr5a1*, *Pax8* and *Aldh1a3* [25]. As the *Plekha5*$^{Tg(AMH-cre)1Flor}$ transgene is not

208 functional in the *rete testis* [26], we anticipated that C20 could comprise cells in which

209 NR5A1 expression was not lost. In agreement, we observed that cells in C20

210 organized as a continuum, which stemmed from C19 with *Nr5a1*⁺/*Yfp*⁻/*Pax8*⁻

211 /*Aldh1a3*⁻ cells and extended with *Nr5a1*⁺/*Yfp*⁻/*Pax8*⁺/*Aldh1a3*⁺ cells (*rete*) originating

212 from both control and *Nr5a1*$^{SC-/-}$ testes. It ended at the junction with C21 with *rete*

213 *testis* cells, originating exclusively from the *Nr5a1*$^{SC-/-}$ testes, and in which cre was

214 active (*Nr5a1*⁻/*Yfp*⁺/*Pax8*⁺/*Aldh1a3*⁺ cells) (**Suppl.Fig.6B**). Accordingly, IHC

215 experiments confirmed that *rete testis* cells actually expressed NR5A1, but not YFP,

216 control and *Nr5a1*$^{SC-/-}$ testes (**Suppl.Fig.6C-J**).

217 **Nr5a1*-deficient SC change their molecular identity.*

218 As indicated above, the NR5A1-deficient SC from cluster C21 gained

219 expression of *Wnt4*, *Fst* and *Rspo1*, which characterize the fetal ovary somatic cells

220 [4]. This raised the question as to whether SC had changed their identity. To test for

221 this possibility, we decided to compare our data with a reference atlas of embryonic

222 and fetal gonad development ranging from E10.5 to E16.5 [25]. After processing this

223   atlas with the pipeline that we used for our data set, (**Suppl.Fig.7**), we next mapped

224   our data set to this reference atlas (**Fig.6A**). Most of control and *Nr5a1*^{SC–/–} cell

225   clusters were predicted to correspond to clusters with identical (or compatible)

226   identities, as expected (**Fig.6B**). In addition, GC from control testes matched in the

227   atlas with E13.5 male GC, while those from *Nr5a1*^{SC–/–} testes matched with E13.5

228   female (i.e., meiotic) GC (**Fig.6C**), as expected from IHC analyses (**Suppl.Fig.5**), and

229   validating thereby the whole prediction. Interestingly, cluster C20 was predicted to

230   match the best with *rete testis* cells, a feature fitting well with our analysis by IHC

231   (see above, **Suppl.Fig.6**). Most importantly, cluster C21 was predicted to correspond

232   to pGrC in the atlas. Further analysis distinguishing the developmental stages

233   indicated that they actually matched with E16.5 pGrC (**Fig.6C**). The remaining cells

234   matched with E13.5 SC. Thus, a fraction of NR5A1-deficient SC lost their identity,

235   and acquired a "pGrC-like" identity. Accordingly, functional analysis of genes

236   differentially expressed by NR5A1-deficient SC assigned upregulated genes to WNT

237   signalling pathway (54 genes, *p* value$<4.3e^{-8}$), known to drive pGrC differentiation in

238   the fetal ovary [27] (**Suppl.Fig.4; Table.S3**). Nonetheless, the process of *trans*-

239   differentiation was not fully achieved because IHC experiments failed to evidence

240   expression of FOXL2 in the *Nr5a1*^{SC–/–} mutant testis at E15.5 (**Fig.6D,E**).

241   ***Ablation of* Nr5a1 *in SC induces disorganisation of the testis cords.***

242   On histological sections at E14.5, the majority of *Nr5a1*^{SC–/–} seminiferous cords

243   displayed reduced diameters, as well as poorly defined and discontinuous contours

244   (broken dotted line and arrows, **Fig.7E**). At E15.5, the cords had almost fully

245   disappeared (broken dotted line, **Fig.7F**). Such irregularities were never observed in

246   the control testes (**Fig.7A,B**).

247   Importantly, functional analysis of the genes differentially expressed between

248   control and NR5A1-deficient SC highlighted extracellular matrix (ECM; 74 genes, *p*

249   value<2.6^{e-16}), cell adhesion (118 genes, *p* value<5.9^{e-9}), basement membrane (26

250   genes, *p* value<2.1^{e-8}), as well as integrin binding (25 genes, *p* value<2.5^{e-6})

251   (**Suppl.Fig.4; Table.S2**). Accordingly, the expression level of some genes involved in

252   cell junction/adhesion (e.g., *Gja1*, *Jam2*, *Ptk2b*) and integrin signalling (e.g., *Itga6*)

253   were down-regulated. As to genes for ECM components, some were down (e.g.,

254   *Col4a1*, *Col4a2*), while many others (e.g., *Col3a1*, *Col5a2*, *Col6a6*, *Fn1*, *Fbln1*, *Mdk*,

255   *Mgp*) were up-regulated (**Fig.7I**). To verify this point, we analysed collagen type IV

256   (COL-IV) expression by IHC. At E14.5, COL-IV was surrounding the whole periphery

257   of all cords in control testes (yellow edging, **Fig.7C**). In *Nr5a1*^{SC–/–}testes, COL-IV was

258   greatly reduced and even absent at the periphery of many cords (arrows, **Fig.7G**), in

259   areas corresponding to regions where the expression of SOX9 was also lost

260   (arrowheads, **Fig.7H**). As *Col4a1* and *Col4a2* are regulated by SOX9 [28], it is

261   reasonable to propose that loss of SOX9 in NR5A1-deficient SC yielded loss of COL-

262   IV and altered basement membrane, which, in turn, disorganized the cord structure.

263   Searching further for ligand-receptor interactions in our data set, we identified a

264   deregulated network related to integrin-dependent cell adhesion (**Suppl.Fig.8**).

265   Together our findings indicate that NR5A1-deficient SC lost their appropriate cell-cell

266   and cell-ECM interactions.

267   **DISCUSSION**

268   Alteration of gene expression in *Nr5a1*^{SC–/–} testes could result from either loss of

269   NR5A1 or death of SC. The decreased expression of *Sox9*, *Amh*, *Gja1*, and possibly

270   *Cyp26b1* and *Dhh*, is likely directly related to the loss of NR5A1 in SC. Actually,

271   NR5A1 initiates SC differentiation by directing *Sox9* expression [9]. Then, it maintains

272 *Sox9* transcription and activates downstream genes by binding to *cis*-regulatory

273 elements (e.g., *Amh*, *Gja1*) or synergizing through unknown mechanisms (e.g.,

274 *Cyp26a1*, *Dhh*) [16,29-32]. As to *Dmrt1*, *Sox8* and *Ptgds*, their decreased expression

275 was also expected because SOX9 regulates their expression [17,31,33,34].

276 However, our finding that *Ptgds* is undetectable as early as E13.5, while SOX9 is still

277 present, suggests that NR5A1 may regulate *Ptgds* expression directly (**Fig.8**).

278 **NR5A1-deficient SC transdifferentiate into pre-granulosa-like cells**

279 Based on genetic studies, SOX9 has emerged as the master regulator

280 instructing SC differentiation during testis development, notably by repressing the

281 WNT4/RSPO1-dependent pathways involved in pGrC differentiation [1-3]. However,

282 human fibroblasts can be reprogramed into SC by forcing expression of NR5A1 and

283 GATA4, but not SOX9 [35]. Here we show that SC lacking NR5A1 from E13.5 loose

284 expression of genes defining or maintaining SC identity (e.g., *Sox9*, *Sox8*, *Ptgds*,

285 *Dmrt1*), further illustrating the primary role of NR5A1 in instructing SC differentiation.

286 In parallel, they gain expression of genes specifying pGrC differentiation (e.g., *Wnt4*,

287 *Rspo1*) and their transcriptome projected to a gonad atlas clearly shows that they

288 display an identity close to that of pGrC. Nonetheless, these "pGrC-like" cannot reach

289 a functional state of differentiation since they keep FOXL2-negative. Another study

290 has shown that SC lacking *Nr5a1* from E12.5 reach a functional, FOXL2-positive,

291 granulosa cell identity, resulting in complete male-to-female sex reversal [36]. This

292 indicates that SC devoid of NR5A1 from E12.5 can transdifferentiate into functional

293 pGrC, while those loosing NR5A1 from E13.5 are no longer licensed to do so. We

294 further show that these "pGrC-like" subsequently die through a *Trp53*-independent

295 mechanism since concomitantly removing *Trp53* and *Nr5a1* does not prevent death.

296 Quite interestingly, SC loosing *Nr5a1* later than E14.5 either die by MDM2/TRP53-

297   dependent apoptosis or survive, since the resulting testis at adulthood still contains

298   clearly defined seminiferous tubules [37]. Thus, the sooner NR5A1 is lost in SC, the

299   highest their plasticity remains, suggesting that NR5A1 progressively locks the SC

300   identity over time. In addition, SC die by distinct mechanisms, depending on the

301   stage at which NR5A1 is lost.

302

303

304   **Sertoli cells lacking NR5A1 from E13.5 die by anoikis**

305   It is accepted that cell adhesion/junction molecules and ECM components play

306   important roles in maintaining the integrity of seminiferous cords [38-40]. Because

307   many genes deregulated in NR5A1-deficient SC are coding for such molecules,

308   including collagen-coding genes, testis cord disruption is likely linked to breakdown of

309   SC adhesion to their environment. Interestingly enough, some of the upregulated

310   genes coding for ECM components such as *Col18a1*, *Fn1*, *Nid2* and *Dcn* (**Table.S2**)

311   are characteristics of pGrC [41].

312   Cells sense their location and maintain their adhesion through specific

313   interactions with the ECM. This plays a major role in regulating various processes,

314   including cell-survival. This function is mediated by integrins, which are the cell-

315   membrane receptors interacting with components of the ECM. They recruit

316   nonreceptor tyrosine focal adhesion kinases (FAK), that are activated in response to

317   adhesion [42]. Therefore, disruption or loss of integrin-ECM adhesion impairs cell-

318   survival, and often causes detachment-induced cell death, called anoikis [43,44]. We

319   found that expression of *Itga6*, an integrin subunit crucial for fetal testis organization

320   [45], and *Ptk2b*, a member of the FAK family expressed in SC in a SOX9-dependent

321   manner [46] is reduced in NR5A1-deficient SC. Thus, it is conceivable that these

322   changes may cause SC to lose their anchorage to the modified ECM (see above)

323   and initiate death of detaching SC by anoikis, altering thereby integrity of the testis

324   cord epithelium (**Fig.8**). It is worth noting that anoikis still occurs in the absence of

325   TRP53 [47], which is fully consistent with our finding that NR5A1-deficient SC die

326   independently of TRP53.

327

328

329   **NR5A1-deficient SC and differentiation of the other testicular cell-types**

330   As to the GC fate, the data show that most of them become meiotic and die in

331   $Nr5a1^{SC-/-}$ testes. The fact that expression of $Cyp26b1$ is lost in NR5A1-deficient SC

332   is sufficient to explain why GC entered meiosis (**Fig.8**). Actually, CYP26B1 is

333   required in SC to prevent meiotic initiation and to maintain GC in an undifferentiated

334   state [48].

335   As to FLC, their specification and/or development rely on SC, notably thanks to

336   DHH- and PDGF-signalling pathways [49,50]. Our finding that FLC are present in

337   $Nr5a1^{SC-/-}$ testes, despite decreased expression of Dhh and $Pdgfa$ in SC, reveals

338   that these pathways are no longer required beyond E13.5 to allow proper emergence

339   or survival of FLC, as observed when SC are ablated after E15.5 [51,52].

340   Furthermore, these FLC appear functional since testicular descent is occurring in

341   $Nr5a1^{SC-/-}$ mutants, suggesting normal INSL3 production [53].

342   As to peritubular myoid cell (PTMC), it is admitted that SC are required during

343   the fetal period to support their differentiation, notably by producing DHH and ECM.

344   Genetic ablation of SC from E14.5 or Dhh-null mutations actually induce seminiferous

345   cords defects closely resembling those observed in *Nr5a1*[SC−/−] testes [54-56]. Thus,

346   the decreased expression of *Dhh* in NR5A1-deficient SC and their death questions

347   the fate of PTMC. As a matter of fact, we could not distinguish PTMC from the

348   interstitial or coelomic epithelium cell clusters. This is not really surprising as PTMC,

349   sparse at E14.5, become obvious only from E16.5 [57], i.e., 2 days later than the

350   stage at which we performed analysis. It is nonetheless worth noting that expression

351   of *Ptch1*, *Tagln*, *Acta2* and *Tpm1*, which are generally considered as hallmarks of

352   PTMC [58,59], were significantly reduced in interstitial or coelomic epithelium cluster

353   cells (**Table.S2**). It is therefore possible that PTMC, included in these clusters, are

354   altered, or even lost, following ablation of *Nr5a1* in SC. Interestingly, both PTMC and

355   "dormant" steroidogenic progenitors (SP) at the origin of adult LC stem from a single

356   population of *Wnt5a*+ SP [60]. In this context, it is conceivable that the absence of

357   adult LC in PND60 testis is related to an alteration of PTMC during fetal

358   development. Further investigations are required to trace the fate of these *Wnt5a*+

359   SP in *Nr5a1*[SC−/−] testis.

Death of the NR5A1-deficient SC affects genital tract development

361   Müllerian duct regression in males proceeds rostro-caudally, and is dependent

362   on the action of AMH, which begins as early as E13.5 [61,62]. As *Amh* expression in

363   *Nr5a1*[SC−/−] mutants is lost only from E14.5, AMH production starts normally and then

364   gradually decreases to zero after E14.5. It is therefore not surprising that the rostral

365   part of the Müllerian ducts regresses normally, making their derivatives (oviducts,

366   anterior portions of the uterine horns absent in the mutants. On the other hand, it is

367   reasonable to propose that the caudal part of the Mullerian ducts persists beyond

368   E14.5, and is at the origin of the posterior portions of the uterine horns, body of the

369   uterus and the vagina of adult *Nr5a1*[SC−/−] mutants (**Fig.8**).

370   In addition, *Nr5a1*SC−/− mutants display normal Wolffian duct-derived genitalia

371   (epididymis, vas deferens, seminal vesicles) [63]. These develop under the influence

372   of testosterone, the synthesis of which starts as early as E13.5 in mice [64]. Their

373   presence indicates therefore that *Nr5a1*SC−/− mutants were exposed to testosterone

374   during fetal development. This is surprising since SC, converting FLC-produced

375   androstenedione into testosterone thanks to expression of *Hsd17b1* and *Hsd17b3*

376   [65], are progressively lost in *Nr5a1*SC−/− mutants. Thus, another enzyme necessarily

377   compensates for the loss of *Hsd17b1* and *Hsd17b3*, as considered elsewhere [66]. In

378   this regard, the HSD17B12 is a good candidate since it can convert androstenedione

379   to testosterone [67]. However, the fact that FLC are not able to produce testosterone

380   from androstenedione [65] means one has to consider HSD17B12 allows

381   testosterone synthesis in a cell-type other than FLC. This production is nevertheless

382   insufficient since AGD and penile bone length, both of which are highly sensitive to

383   testosterone levels between E14.5 and E17.5 in mice [68], are reduced in *Nr5a1*SC−/−

384   mutants (**Fig.8**).

385   Our study shows that SC lacking NR5A1 from E13.5 transiently

386   transdifferentiate to acquire a pre-granulosa cell-like identity, profoundly modify the

387   landscape of the adhesion molecules and ECM they express and die by a TRP53-

388   independent mechanism related to anoikis. This yields a disorganization of the testis

389   cords, making GC to prematurely enter meiosis instead of becoming quiescent.

390   Interestingly, the maintenance of fetal LC is not altered in the *Nr5a1*SC−/− mutant, but

391   the emergence of adult LC is clearly compromised. Further studies are now required

392   to understand the reason for the absence of adult LC in the postnatal testis.

393   **MATERIALS AND METHODS**

394   **Mice**

395   They were on a mixed C57BL/6 (50%)/129/SvPass (50%) genetic background.

396   The *Nr5a1* conditional mutant mouse line was established at the Institut Clinique de

397   la Souris (*i*CS, Illkirch, France), in the context of the French National Infrastructure for

398   Mouse Phenogenomics PHENOMIN (http://www.phenomin.fr). To construct the

399   targeting vector a 1.9 kb-long DNA fragment encompassing exon 7

400   (ENSMUSE00000 693512) was amplified by PCR using 129/SvPass genomic DNA

401   and cloned into an *i*CS proprietary vector containing a *lox*P site, as well as a *lox*P-

402   and *FRT*-flanked neomycin resistance cassette (step1 plasmid). Then, 3 kb- and

403   3.7 kb-long fragments corresponding to 5' and 3' homology arms were amplified by

404   PCR and introduced into step1 plasmid to generate the targeting construct. This

405   linearized construct was electroporated into 129/SvPass mouse embryonic stem (ES)

406   cells. After selection, targeted clones were identified by PCR using external primers

407   and confirmed by Southern blots (5' and 3' digests) hybridized with neomycin, 5' and

408   3' external probes. One positive ES clone was injected into C57BL/6J blastocysts. To

409   remove the selection cassette from the *Nr5a1* locus, chimeric males were crossed

410   with *Gt(ROSA)26Sor*$^{tm1(FLP1)Dym}$ females [69]. Germline transmission was obtained,

411   and a further breeding step was needed to segregate animals bearing the *Nr5a1* L2

412   allele from animals bearing the transgene. To inactivate *Nr5a1* in SC, female mice

413   bearing *Plekha5*$^{Tg(AMH-cre)1Flor}$ [14] and *Gt(ROSA)26Sor*$^{tm1(EYFP)Cos}$ [15] transgenes,

414   and heterozygous for the L2 allele of *Nr5a1* were mated with males heterozygous or

415   homozygous for L2 alleles of *Nr5a1*. The resulting *Plekha5*$^{Tg(AMH-cre)1Flor}$;*Nr5a1*$^{+/+}$;

416   *Gt(ROSA)26Sor*$^{tm1(EYFP)Cos}$ and *Plekha5*$^{Tg(AMH-cre)1Flor}$;*Nr5a1*$^{L2/L2}$; *Gt(ROSA)26Sor*$^{tm1(EYFP)Cos}$

417   males are referred to as control and *Nr5a1*$^{SC-/-}$ mutant fetuses, respectively. To test

418   for the role of TRP53, the L2 allele of *Trp53* gene [21] was further introduced in the

419   mice described above.

420   Noon of the day of a vaginal plug was taken as 0.5 day embryonic development

421 (E0.5). All fetuses were collected by caesarean section (no randomization, no blind

422 experiments). Yolk sacs or tail biopsies were taken for DNA extraction. Primers 5'-

423 GTCAAGCGCCCCATGAATGC-3' and 5'-TTAGCCCTCCGATGAGGCTG-3' were

424 first used to amplify *Sry* gene (230 bp-long fragment) for male sex determination.

425 Then, primers 5'-TGAGCCCTGGCACATCCCTCC-3' and 5'-

426 CCTCTGCCCTGCAGGCTTC TG-3' were used to detect *Plekha5*^{Tg(AMH-cre)1Flor}

427 transgene (273 bp-long amplicon), and primers 5'-AAGGGAGCTGCAGTGGAGTA-3'

428 and 5'-GCCAGAGGCCACTTGTGTAG-3' to detect *Gt(ROSA)26Sor*^{tm1(EYFP)Cos}

429 reporter (520 bp-long amplicon). Primers 5'-CTGTCTCCTGTCTTCTACTACCCTG-3'

430 and 5'-AGCCATTTCAACAGTGCCCC TTCC-3' were used to amplify wild-type (+,

431 290 bp-long) and L2 (400 bp-long) alleles of *Nr5a1*, while primers 5'-

432 GTGGCACATGCATTAGTCCACTTGG-3' and 5'-

433 AGCCATTTCAACAGTGCCCCTTCC-3' were used to amplify the excised, null, L–

434 (243 bp-long) allele. Primers 5'-CACAAAAACAGGTTAAACCCAG-3' and 5'-

435 AGCACATAGGAGGCAGAGAC-3' were used to amplify the wild-type (288 bp-long)

436 and L2 (370 bp-long) alleles of *Trp53*. Primers 5'-CACAAAAACAGGTTAAACCCAG-

437 3' and 5'-GAAGACAGAAAAGGGGAG GG-3' were used to amplify the excised, null,

438 L– (612 bp-long) allele of *Trp53*. The PCR conditions were 30 cycles with

439 denaturation at 95°C for 30 seconds, annealing at 61°C for 30 seconds and

440 elongation at 72°C for 30 seconds. The amplicons were resolved on 1.5% (w/v)

441 agarose gels, stained by ethidium bromide and visualized under UV light, using

442 standard protocols.

443 **Blood sample collection and testosterone measurement**

444   After anesthesia with a lethal dose of Xylasin and Ketamine as described

445   above, the blood of 9-11-week-old adult mice was collected into heparinized

446   Microvette tubes (Sarstedt, Nümbrecht, Germany) by intra-cardiac sampling. The

447   tubes were then centrifuged at 5000 g for 5 minutes and the resulting plasma

448   samples were frozen until further use. Testosterone concentrations were determined

449   by ELISA using a commercially available kit AR E-8000 (LDN, Labor Diagnostika

450   Nord, Nordhorn, Germany). Statistical significance was further assessed by using

451   two-tail Student's *t*-tests.

Morphology, histology and immunohistochemistry

453   Adult mice (PND60) were anesthetized by intraperitoneal injection of a lethal

454   anesthetic mixture made of Xylasin (3 mg/ml) and Ketamine (20 mg/ml), and tissues

455   were immediately fixed by intracardiac perfusion of 4% (w/v) paraformaldehyde

456   (PFA) dissolved in phosphate buffered saline (PBS). Following collection, E12.5-

457   E15.5 fetuses and tissues were fixed for 16 hours in 4% (w/v) PFA at 4°C or in

458   Bouin's fluid at 20°C. After removal of the fixative, samples were rinsed in PBS and

459   placed in 70% (v/v) ethanol for long-term storage, external morphology evaluation

460   and organ weight measurement. They were next embedded in paraffin and 5 µm-

461   thick sections were made. For histology, sections were stained with hematoxylin and

462   eosin (H&E).

463   For IHC, antigens were retrieved for 1 hour at 95°C either in 10 mM sodium

464   citrate buffer at pH 6.0 or in Tris-EDTA at pH 9.0 [10 mM Tris Base, 1 mM EDTA,

465   0.05% (v/v) Tween 20]. Sections were rinsed in PBS, then incubated with appropriate

466   dilutions of the primary antibodies (**Table.1**) in PBS containing 0.1% (v/v) Tween 20

467   (PBST) for 16 hours at 4°C in a humidified chamber. After rinsing in PBST (3 times

468   for 3 minutes each), detection of the bound primary antibodies was achieved for

469   45 minutes at 20°C in a humidified chamber using Cy3-conjugated or Alexa Fluor

470   488-conjugated antibodies. Nuclei were counterstained with 4',6-diamidino-2-phenyl-

471   indole (DAPI) diluted at 10 µg/ml in the mounting medium (Vectashield; Vector

472   Laboratories, Newark, CA, USA). ImmPRESS® Polymer Detection Kits MP-7500 and

473   MP-7405 were used according to the manufacturer's protocol (Vector Laboratories).

474   The surface area occupied by YFP-positive cells was measured using a macro

475   command designed for Fiji software (Imaging Center of IGBMC). Data were

476   expressed as percentage of YFP-positive surface areas relative to the entire testis

477   section surface areas. At least four samples were analyzed per genotype. Statistical

478   analysis was done by a two-tail Student *t*-test, assuming equal variances after

479   arcsine transformation of the percentages.

480

481

482   **BrdU incorporation and TUNEL assays**

483   BrdU (Sigma-Aldrich, Saint-Quentin-Fallavier, France) dissolved at 5 mg/ml in

484   PBS was injected intraperitoneally to pregnant females at 50 mg/kg of body weight.

485   Two hours later, fetuses were collected (E13.5-E15.5), fixed and embedded as

486   described above. BrdU incorporation was detected on 5 µm-thick sections by using

487   an anti-BrdU mouse monoclonal antibody (diluted 1:100) and indirect IHC as

488   described above. At least three samples per stage and per genotype were analyzed.

489   Data were expressed as percentages of BrdU-positive cells related to the number of

490   DDX4-positive cells. Statistical analysis was done by a two-tail Student *t*-test,

491   assuming equal variances after arcsine transformation of the percentages.

492   TUNEL-positive cells were detected on sections from PFA-fixed samples using

493   the In Situ Cell Death Detection Kit, Fluorescein, according to the manufacturer's

494   instructions (Roche, Mannheim, Germany). At least three samples were analyzed per

495   genotype. Data were expressed as the ratio between the number of TUNEL-positive

496   cells quantified on entire sections and the surface areas of the testis sections (μm^2).

497   Statistical significance was assessed by using two tail Student's *t*-tests.

498   **Real-time RT-qPCR analyses of RNA extracted from whole gonad**

499   Fetal testes were dissected, isolated from mesonephros, snap frozen in liquid

500   nitrogen and stored at –80°C until use. Whole testis total RNA was extracted using

501   RNeasy Mini Kit (Qiagen, Les Ulis, France). RT-qPCR was performed on 5 ng RNA

502   aliquots using Luna® Universal One-Step RT-qPCR Kit, according to the

503   manufacturer's instructions (New England Biolabs, Evry, France). The primers are

504   listed in **Table.2**. Triplicates of at least four samples were used for each genotype, at

505   each stage. The relative transcript levels were determined using the ΔΔCt method,

506   and normalized to *Hprt* whose expression is not affected by ablation of *Nr5a1*.

507   **Purification of YFP-positive Sertoli cells**

508   To dissociate cells, the testes of controls and mutants additionally bearing the

509   *Gt(ROSA)26Sor*^tm1(EYFP)Cos^ transgene were incubated for 10 minutes at 37°C in

510   350 µl of trypsin/EDTA 0.05% (w/v), phenol red solution (Gibco Invitrogen, Auckland,

511   New-Zealand), filtered through a 40 µm cell strainer to generate single cell

512   suspensions, centrifuged at 3000g and suspended in 300 µl PBS as described [70].

513   The YFP-positive and -negative cells were sorted separately by FACS using an

514   Aria® II flow cytometer (BD Biosciences, Le Pont de Claix, France). Sorted cell

515   suspensions were then lysed for overnight at 55°C in a proteinase K-containing

516   buffer, DNA was extracted and genotyped by PCR using standard protocols and

517   primers as indicated above.

Single cell RNA sequencing and data processing

519   Gonads from E13.5 and E14.5 control and mutant fetuses were dissected out in

520   PBS, sexed by their appearance under the microscope and cell suspensions were

521   prepared as described above. Cell number and viability were determined by a Trypan

522   Blue exclusion assay on a Neubauer Chamber. Samples consisting of > 90% viable

523   cells were processed on the Chromium Controller from 10X Genomics (Leiden, The

524   Netherlands). Ten thousand cells were loaded per well to yield approximately 5000 to

525   6000 captured cells into nanoliter-scale Gel Beads-in-Emulsion (GEMs). Single cell 3'

526   mRNA sequencing libraries were generated according to Chromium Single Cell 3'

527   Reagent Kits User Guide (v3 Chemistry) from 10X Genomics. Briefly, GEMs were

528   generated by combining barcoded gel beads, a reverse transcription master mix

529   containing cells, and partitioning oil onto Chromium Chip B. Following full length

530   cDNA synthesis and barcoding from poly-adenylated mRNA, GEM were broken and

531   pooled before cDNA amplification by PCR using 11 cycles. After enzymatic

532   fragmentation and size selection, sequencing libraries were constructed by adding

533   Illumina P5 and P7 primers (Illumina, Evry, France), as well as sample index via end

534   repair, A tailing, adaptor ligation and PCR with 10 cycles. Library quantifications and

535   quality controls were determined using Bioanalyzer 2100 (Agilent Technologies,

536   Santa Clara, CA, USA). Libraries were then sequenced on Illumina HiSeq 4000™ as

537   100 bases paired-end reads, using standard protocols.

538   Sequencing data were processed using 10X Genomics software

539   (https://support.10xgenomics.com/single-cell-gene-expression/software/overview/welcome).

540   Fastq files were processed with CellRanger (v6.0) on a chimeric genome composed

541   of mm10 *Mus musculus* assembly and 753 bp-long YFP sequence (European

542   Nucleotide Archive accession number AGM20711) [71]. The resulting count matrices

543   were aggregated with the Read10X function implemented in Seurat (v4.0.1) [72].

544   Cells with less than 200 detected genes and genes detected in less than 10 cells

545   were removed. Doublets were filtered out independently in each individual matrix by

546   using the DoubletFinder R package (v.2.0.2) [73]. Subsequently, the Single-Cell

547   Analysis Toolkit for Gene Expression Data in R (scater v1.10.1) was used to remove

548   outlier cells by using several cell features including the proportions of reads mapping

549   mitochondrial and ribosomal genes, the number of genes and UMIs per cell [74].

550   Data were normalized using the NormalizeData and the SCT function implemented

551   into Seurat by regressing out the unwanted variation due to cell cycle and to the

552   proportion of mitochondrial genes. The top-3000 most varying genes were used to

553   perform a principal component analysis with the RunPCA function implemented in

554   Seurat. Cells were then clustered by using Seurat graph-based clustering

555   (FindNeighbors and FindClusters functions) on the top-30 principal components, with

556   default parameters. Finally, we used the Uniform Manifold Approximation and

557   Projection (UMAP) method (RunUMAP function) to project cells in a 2D space. Cell

558   clusters were annotated using a set of known marker genes. The FindAllMarkers

559   function implemented in Seurat was used to identify significantly differentially

560   expressed genes (DEGs) between cell clusters. Gene ontology (GO) and pathway

561   enrichment analysis was conducted for each gene expression cluster using the

562   AMEN suite of tools [75] with an BH-adjusted p value of ≤ 0.05. The current dataset

563   was mapped on top of a reference atlas of gonadal development [25] using

564   FindTransferAnchors and MapQuery functions with default settings. To address this

565   issue, the reference atlas was first processed by using the same pipeline.

ACKNOWLEDGEMENTS

566

567   The *Nr5a1* mouse mutant line was established at the Institut Clinique de la

568   Souris (PHENOMIN *i*CS) in the Genetic Engineering and Model Validation

569   Department with funds from the ANR (see below). We thank Pr Anne-Marie

570   LEFRANCOIS-MARTINEZ for discussions and advices. We also thank Dr Christelle

571   Thibault-CARPENTIER from the Genomeast platform for her input

572   (http://genomeast.igbmc.fr/). This research was funded by Agence Nationale pour la

573   Recherche Grants (see below). A CC-BY-4.0 public copyright license has been

574   applied by the authors to the present document and will be applied to all subsequent

575   versions up to the Author Accepted Manuscript arising from this submission, in

576   accordance with the grant's open access conditions.

FUNDING

577

578   This work was supported by grants from Fondation pour la Recherche Médicale

579   (FRM FDT201904008001), CNRS, INSERM, UNISTRA and Agence Nationale pour

580   la Recherche project ARESSERC (ANR-16-CE14-0017). It was also supported in

581   part by the grant ANR-10-LABX-0030-INRT, a French State fund managed by the

582   ANR under the frame Programme Investissements d'Avenir labelled ANR-10-IDEX-

583   0002-02.

AUTHOR INFORMATION

584

585   These authors contributed equally: Frédéric Chalmel, Norbert B. Ghyselinck.

Contributions

586

587   SSC, MM and NBG conceptualized and designed the study. SSC and DC

588   performed all the experiments. BF and MK provided technical and material support.

589   EG contributed to image analysis. SSC, VA, MC, MJ and FC performed the scRNA-

590   seq experiment and analysed data. CM and SN provided datasets for the mouse

591   gonad atlas. SSC, NV, MM, FC and NBG analysed all experiments, managed the

592   overall study, wrote the manuscript, and supervised its preparation and submission.

593   NV, MM, FC and NBG acquired funding for this research.

594   **Corresponding authors**

595   Correspondence to Norbert B. Ghyselinck.

596   **ETHICS DECLARATIONS**

597   **Competing interests**

598   The authors declare no competing interests.

599   **Ethics statement**

600   Mice were housed in a licensed animal facility (agreement #C6721837). All

601   experiments were approved by the local ethical committee (Com'Eth, accreditation

602   APAFIS#18323- 2018113015272439_v3), and were supervised by N.B.G., M.M. and

603   N.V., who are qualified in compliance with the European Community guidelines for

604   laboratory animal care and use (2010/63/UE).

605   **DATA AVAILABILITY**

606   The data sets described in this paper are available at Gene Expression

607   Omnibus (GEO) database under the accession number GSE219271.

608   **SUPPLEMENTARY INFORMATION**

609   Supplementary information is available at *Cell Death and Differentiation*'s

610   website.

611   **REFERENCES**

612   1. Yao HH, Ungewitter E, Franco H & Capel B. Establishment of fetal Sertoli cells

613   and their role in testis morphogenesis. In: Griswold MD (ed). Sertoli Cell Biology.

614   2nd edn.   (Academic   Press,   Cambridge,   2015)   57-79.

615   https://doi.org/10.1016/B978-0-12-417047-6.00002-8

616   2. Rotgers E, Jørgensen A & Yao HH. At the Crossroads of Fate-Somatic Cell

617   Lineage Specification in the Fetal Gonad. *Endocr Rev* **39**, 739-759 (2018)

618   PMID:29771299

619   3. Nef S, Stévant I & Greenfield A. Characterizing the bipotential mammalian

620   gonad. *Curr Top Dev Biol* **134**, 167-194 (2019) PMID:30999975

621   4. Eggers S, Ohnesorg T & Sinclair A. Genetic regulation of mammalian gonad

622   development. *Nat Rev Endocrinol* **10**, 673-683 (2014) PMID:25246082

623   5. Fabbri-Scallet H, de Sousa LM, Maciel-Guerra AT, Guerra-Júnior G & de Mello

624   MP. Mutation update for the NR5A1 gene involved in DSD and infertility. *Hum*

625   *Mutat* **41**, 58-68 (2020) PMID:31513305

626   6. Morohashi K, Baba T & Tanaka M. Steroid hormones and the development of

627   reproductive organs. *Sex Dev* **7**, 61-79 (2013) PMID:22986257

628   7. Morohashi KI, Inoue M & Baba T. Coordination of Multiple Cellular Processes by

629   NR5A1/Nr5a1. *Endocrinol Metab (Seoul)* **35**, 756-764 (2020) PMID:33397036

630   8. Luo X, Ikeda Y & Parker KL. A cell-specific nuclear receptor is essential for

631   adrenal and gonadal development and sexual differentiation. *Cell* **77**, 481-490

632   (1994) PMID:8187173

633   9. Sekido R & Lovell-Badge R. Sex determination involves synergistic action of

634   SRY and SF1 on a specific Sox9 enhancer. *Nature* **453**, 930-934 (2008)

635   PMID:18454134

636   10. Cool J, DeFalco T & Capel B. Testis formation in the fetal mouse: dynamic and

637   complex de novo tubulogenesis. *Wiley Interdiscip. Rev Dev Biol* **1**, 847-859

638   (2012) PMID:23799626

639   11. Griswold MD. 50 years of spermatogenesis: Sertoli cells and their interactions

640   with germ cells. *Biol Reprod* **99**, 87-100 (2018) PMID:29462262

641   12. Bitgood MJ, Shen L & McMahon AP. Sertoli cell signaling by Desert hedgehog

642   regulates the male germline. *Curr Biol* **6**, 298-304 (1996) PMID:8805249

643   13. Josso N & Picard JY. Genetics of anti-Müllerian hormone and its signaling

644   pathway. *Best Pract Res Clin Endocrinol Metab* **36**, 101634 (2022)

645   PMID:35249805

646   14. Lécureuil C, Fontaine I, Crepieux P & Guillou F. Sertoli and granulosa cell-

647   specific Cre recombinase activity in transgenic mice. *Genesis* **33**, 114-118 (2002)

648   PMID:12124943

649   15. Srinivas S, Watanabe T, Lin CS, William CM, Tanabe Y, Jessell TM *et al.* Cre

650   reporter strains produced by targeted insertion of EYFP and ECFP into the

651   ROSA26 locus. *BMC Dev Biol* **1**, 4 (2001) PMID:11299042

652   16. De Santa Barbara P, Bonneaud N, Boizet B, Desclozeaux M, Moniot B, Sudbeck

653   P *et al.* Direct interaction of SRY-related protein SOX9 and steroidogenic factor

654   1 regulates transcription of the human anti-Müllerian hormone gene. *Mol Cell Biol*

655   **18**, 6653-6665 (1998) PMID:9774680

656   17. Wilhelm D, Hiramatsu R, Mizusaki H, Widjaja L, Combes AN, Kanai Y *et al.*

657   SOX9 regulates prostaglandin D synthase gene transcription in vivo to ensure

658   testis development. *J Biol Chem* **282**, 10553-10560 (2007) PMID:17277314

659   18. Malki S, Nef S, Notarnicola C, Thevenet L, Gasca S, Méjean C *et al*.

660   Prostaglandin D2 induces nuclear import of the sex-determining factor SOX9 via

661   its cAMP-PKA phosphorylation. *EMBO J* **24**, 1798-1809 (2005) PMID:15889150

662   19. Tremblay JJ & Viger RS. Transcription factor GATA-4 enhances Müllerian

663   inhibiting substance gene transcription through a direct interaction with the

664   nuclear receptor SF-1. *Mol Endocrinol* **13**, 1388-1401 (1999) PMID:10446911

665   20. Buganim Y, Itskovich E, Hu YC, Cheng AW, Ganz K, Sarkar S *et al*. Direct

666   reprogramming of fibroblasts into embryonic Sertoli-like cells by defined factors.

667   *Cell Stem Cell* **11**, 373-386 (2012) PMID:22958931

668   21. Jonkers J, Meuwissen R, van der Gulden H, Peterse H, van der Valk M & Berns

669   A. Synergistic tumor suppressor activity of BRCA2 and p53 in a conditional

670   mouse model for breast cancer. *Nat Genet* **29**, 418-425 (2001) PMID:11694875

671   22. Sararols P, Stévant I, Neirijnck Y, Rebourcet D, Darbey A, Curley MK *et al*.

672   Specific Transcriptomic Signatures and Dual Regulation of Steroidogenesis

673   Between Fetal and Adult Mouse Leydig Cells. *Front Cell Dev Biol* **9**, 695546

674   (2021) PMID:34262907

675   23. Welsh M, Suzuki H & Yamada G. The masculinization programming window.

676   *Endocr Dev* **27**, 17-27 (2014) PMID:25247641

677   24. Kulibin AY & Malolina EA. Formation of the rete testis during mouse embryonic

678   development. *Dev Dyn* **249**, 1486-1499 (2020) PMID:32852840

679   25. Mayère C, Regard V, Perea-Gomez A, Bunce C, Neirijnck Y, Djari C *et al*.

680   Origin, specification and differentiation of a rare supporting-like lineage in the

681   developing mouse gonad. *Sci Adv* **8**, eabm0972 (2022) PMID:35613264

682   26. Teletin M, Vernet N, Yu J, Klopfenstein M, Jones JW, Féret B *et al*. Two functionally redundant sources of retinoic acid secure spermatogonia differentiation in the seminiferous epithelium. *Development* **146**, dev170225 (2019) PMID:30487180

686   27. Chassot AA, Gillot I & Chaboissier MC. R-spondin1, WNT4, and the CTNNB1 signaling pathway: strict control over ovarian differentiation. *Reproduction* **148**, R97-110 (2014) PMID:25187620

689   28. Sumi E, Iehara N, Akiyama H, Matsubara T, Mima A, Kanamori H *et al*. SRY-related HMG box 9 regulates the expression of Col4a2 through transactivating its enhancer element in mesangial cells. *Am J Pathol* **170**, 1854-1864 (2007) PMID:17525254

693   29. Arango NA, Lovell-Badge R & Behringer RR. Targeted mutagenesis of the endogenous mouse Mis gene promoter: in vivo definition of genetic pathways of vertebrate sexual development. *Cell* **99**, 409-419 (1999) PMID:10571183

696   30. Kashimada K, Svingen T, Feng CW, Pelosi E, Bagheri-Fam S, Harley VR *et al*. Antagonistic regulation of Cyp26b1 by transcription factors SOX9/SF1 and FOXL2 during gonadal development in mice. *FASEB J* **25**, 3561-3569 (2011) PMID:21757499

700   31. Li Y, Zheng M & Lau YF. The sex-determining factors SRY and SOX9 regulate similar target genes and promote testis cord formation during testicular differentiation. *Cell Rep* **8**, 723-733 (2014) PMID:25088423

703   32. Couture R & Martin LJ. The transcription factors SF-1 and SOX8 cooperate to upregulate Cx43 expression in mouse TM4 sertoli cells. *Biochem Biophys Rep* **24**, 100828 (2020) PMID:33088929

706   33. Chaboissier MC, Kobayashi A, Vidal VI, Lützkendorf S, van de Kant HJ, Wegner

707   M *et al.* Functional analysis of Sox8 and Sox9 during sex determination in the

708   mouse. *Development* **131**, 1891-1901 (2004) PMID:15056615

709   34. Rahmoun M, Lavery R, Laurent-Chaballier S, Bellora N, Philip GK, Rossitto M *et*

710   *al.* In mammalian foetal testes, SOX9 regulates expression of its target genes by

711   binding to genomic regions with conserved signatures. *Nucleic Acids Res* **45**,

712   7191-7211 (2017) PMID:28472341

713   35. Liang J, Wang N, He J, Du J, Guo Y, Li L *et al.* Induction of Sertoli-like cells from

714   human fibroblasts by NR5A1 and GATA4. *Elife* **8**, e48767 (2019)

715   PMID:31710289

716   36. Ikeda Y, Tagami A, Maekawa M & Nagai A. The conditional deletion of

717   steroidogenic factor 1 (Nr5a1) in Sox9-Cre mice compromises testis

718   differentiation. Sci Rep **11**, 4486 (2021) PMID:33627800

719   37. Anamthathmakula P, Miryala CSJ, Moreci RS, Kyathanahalli C, Hassan SS,

720   Condon JC *et al.* Steroidogenic Factor 1 (Nr5a1) is Required for Sertoli Cell

721   Survival Post Sex Determination. *Sci Rep* **9**, 4452 (2019) PMID:30872705

722   38. Barrionuevo F, Georg I, Scherthan H, Lécureuil C, Guillou F, Wegner M *et al.*

723   Testis cord differentiation after the sex determination stage is independent of

724   Sox9 but fails in the combined absence of Sox9 and Sox8. *Dev Biol* **327**, 301-312

725   (2009) PMID:19124014

726   39. Georg I, Barrionuevo F, Wiech T & Scherer G. Sox9 and Sox8 are required for

727   basal lamina integrity of testis cords and for suppression of FOXL2 during

728   embryonic testis development in mice. *Biol Reprod* **87**, 99 (2012)

729   PMID:22837482

730   40. Chen SR, Chen M, Wang XN, Zhang J, Wen Q, Ji SY *et al*. The Wilms tumor
731   gene, Wt1, maintains testicular cord integrity by regulating the expression of
732   Col4a1 and Col4a2. *Biol Reprod* **88**, 56 (2013) PMID:23325811

733   41. Piprek RP, Kolasa M, Podkowa D, Kloc M & Kubiak JZ. Transcriptional profiling
734   validates involvement of extracellular matrix and proteinases genes in mouse
735   gonad development. *Mech Dev* **149**, 9-19 (2018) PMID:29129619

736   42. Lu Q & Rounds S. Focal adhesion kinase and endothelial cell apoptosis.
737   *Microvasc Res* **83**, 56-63 (2012) PMID:21624380

738   43. Gilmore AP. Anoikis. *Cell Death Differ* **12 Suppl 2**, 1473-1477 (2005)
739   PMID:16247493

740   44. Vachon PH. Integrin signaling, cell survival, and anoikis: distinctions, differences,
741   and differentiation. *J Signal Transduct* **2011**, 738137 (2011) PMID:21785723

742   45. Fröjdman K & Pelliniemi LJ. Differential distribution of the alpha 6 subunit of
743   integrins in the development and sexual differentiation of the mouse testis.
744   *Differentiation* **57**, 21-29 (1994) PMID:8070619

745   46. Beverdam A, Svingen T, Bagheri-Fam S, McClive P, Sinclair AH, Harley VR *et al*.
746   Protein tyrosine kinase 2 beta (PTK2B), but not focal adhesion kinase (FAK), is
747   expressed in a sexually dimorphic pattern in developing mouse gonads. *Dev Dyn*
748   **239**, 2735-2741 (2010) PMID:20737507

749   47. McGill G, Shimamura A, Bates RC, Savage RE & Fisher DE. Loss of matrix
750   adhesion triggers rapid transformation-selective apoptosis in fibroblasts. *J Cell*
751   *Biol* **138**, 901-911 (1997) PMID:9265655

752   48. Li H, MacLean G, Cameron D, Clagett-Dame M & Petkovich M. Cyp26b1
753   expression in murine Sertoli cells is required to maintain male germ cells in an

754   undifferentiated state during embryogenesis. *PLoS One* **4**, e7501 (2009)

755   PMID:19838304

756   49. Yao HH, Whoriskey W & Capel B. Desert Hedgehog/Patched 1 signaling

757   specifies fetal Leydig cell fate in testis organogenesis. *Genes Dev* **16**, 1433-1440

758   (2002) PMID:12050120

759   50. Brennan J, Tilmann C & Capel B. Pdgfr-alpha mediates testis cord organization

760   and fetal Leydig cell development in the XY gonad. *Genes Dev* **17**, 800-810

761   (2003) PMID:1265189

762   51. Rebourcet D, O'Shaughnessy PJ, Pitetti JL, Monteiro A, O'Hara L, Milne L *et al.*

763   Sertoli cells control peritubular myoid cell fate and support adult Leydig cell

764   development in the prepubertal testis. *Development* **141**, 2139-2149 (2014)

765   PMID:24803659

766   52. Fouchécourt S, Livera G, Messiaen S, Fumel B, Parent AS, Marine JC *et al.*

767   Apoptosis of Sertoli cells after conditional ablation of murine double minute 2

768   (Mdm2) gene is p53-dependent and results in male sterility. *Cell Death Differ* **23**,

769   521-530 (2016) PMID:26470726

770   53. Verma-Kurvari S, Nef S & Parada LF. Hormonal regulation of male reproductive

771   tract development. *Ann N Y Acad Sci* **1061**, 1-8 (2005) PMID:16467252

772   54. Clark AM, Garland KK & Russell LD. Desert hedgehog (Dhh) gene is required in

773   the mouse testis for formation of adult-type Leydig cells and normal development

774   of peritubular cells and seminiferous tubules. *Biol Reprod* **63**, 1825-1838 (2000)

775   PMID:11090455

776   55. Pierucci-Alves F, Clark AM & Russell LD. A developmental study of the Desert

777   hedgehog-null mouse testis. *Biol Reprod* **65**, 1392-1402 (2001) PMID:1167325

778   56. Wang YQ, Cheng JM, Wen Q, Tang JX, Li J, Chen SR *et al*. An exploration of the

779   role of Sertoli cells on fetal testis development using cell ablation strategy. *Mol*

780   *Reprod Dev* **87**, 223-230 (2020) PMID:32011766

781   57. Aksel S, Cao M, Derpinghaus A, Baskin LS & Cunha GR. Ontogeny of mouse

782   Sertoli, Leydig and peritubular myoid cells from embryonic day 10 to adulthood.

783   *Differentiation* **Mar7**, S0301-4681(22)00015-9 (2022) PMID:35317954

784   58. Jeanes A, Wilhelm D, Wilson MJ, Bowles J, McClive PJ, Sinclair AH *et al*.

785   Evaluation of candidate markers for the peritubular myoid cell lineage in the

786   developing mouse testis. *Reproduction* **130**, 509-516 (2005) PMID:16183868

787   59. Sohni A, Tan K, Song HW, Burow D, de Rooij DG, Laurent L *et al*. The Neonatal

788   and Adult Human Testis Defined at the Single-Cell Level. *Cell Rep* **26**, 1501-

789   1517.e4 (2019). PMID:30726734

790   60. Ademi H, Djari C, Mayère C, Neirijnck Y, Sararols P, Rands CM *et al*.

791   Deciphering the origins and fates of steroidogenic lineages in the mouse testis.

792   *Cell Rep* **39**, 110935 (2022). PMID:35705036

793   61.Staack A, Donjacour AA, Brody J, Cunha GR & Carroll P. Mouse urogenital

794   development: a practical approach. *Differentiation* **71**, 402-413 (2003)

795   PMID:12969333

796   62. Mullen RD & Behringer RR. Molecular genetics of Müllerian duct formation,

797   regression and differentiation. *Sex Dev* **8**, 281-296 (2014) PMID:25033758

798   63. Zhao F & Yao HH. A tale of two tracts: history, current advances, and future

799   directions of research on sexual differentiation of reproductive tracts. *Biol Reprod*

800   **101**, 602-616 (2019) PMID:31058957

801   64. Livera G, Delbes G, Pairault C, Rouiller-Fabre V & Habert R. Organotypic culture,

802   a powerful model for studying rat and mouse fetal testis development. *Cell Tissue*

803   *Res* **324**, 507-521 (2006). PMID:16520975

804   65. Shima Y, Miyabayashi K, Haraguchi S, Arakawa T, Otake H, Baba T *et al*.

805   Contribution of Leydig and Sertoli cells to testosterone production in mouse fetal

806   testes. *Mol Endocrinol* **27**, 63-73 (2013) PMID:23125070

807   66. Rebourcet D, Mackay R, Darbey A, Curley MK, Jørgensen A, Frederiksen H *et*

808   *al*. Ablation of the canonical testosterone production pathway via knockout of the

809   steroidogenic enzyme HSD17B3, reveals a novel mechanism of testicular

810   testosterone production. *FASEB J* **34**, 10373-10386 (2020) PMID:32557858

811   67. Blanchard PG & Luu-The V. Differential androgen and estrogen substrates

812   specificity   in   the   mouse   and   primates   type   12   17beta-hydroxysteroid

813   dehydrogenase. *J Endocrinol* **194**, 449-455 (2007) PMID:17641292

814   68. Welsh M, Suzuki H & Yamada G. The masculinization programming window.

815   *Endocr Dev* **27**, 17-27 (2014) PMID:25247641

816   69. Farley FW, Soriano P, Steffen LS, Dymecki SM.   Widespread recombinase

817   expression using FLPeR (flipper) mice. *Genesis* **28**, 106-110 (2000) PMID:

818   11105051

819   70. Stévant I, Neirijnck Y, Borel C, Escoffier J, Smith LB, Antonarakis SE *et al*.

820   Deciphering Cell Lineage Specification during Male Sex Determination with

821   Single-Cell RNA Sequencing. *Cell Rep* **22**, 1589-1599 (2018) PMID:29425512

822   71. Aliye N, Fabbretti A, Lupidi G, Tsekoa T & Spurio R. Engineering color variants

823   of   green   fluorescent   protein   (GFP)   for   thermostability,   pH-sensitivity,   and

824   improved folding kinetics. *Appl Microbiol Biotechnol* **99**, 1205-1216 (2015)

825   PMID:25112226.

826   72. Hao Y, Hao S, Andersen-Nissen E, Mauck WM 3rd, Zheng S, Butler A *et al.*

827   Integrated analysis of multimodal single-cell data. *Cell* **184**, 3573-3587 (2021)

828   PMID: 34062119

829   73. McGinnis CS, Murrow LM & Gartner ZJ. DoubletFinder: Doublet Detection in

830   Single-Cell RNA Sequencing Data Using Artificial Nearest Neighbors. *Cell Syst* **8**,

831   329-337 (2019) PMID:30954475

832   74. McCarthy DJ, Campbell KR, Lun AT & Wills QF. Scater: pre-processing, quality

833   control, normalization and visualization of single-cell RNA-seq data in R.

834   *Bioinformatics* **33**, 1179-1186 (2017). PMID:28088763

835   75. Chalmel F & Primig M. The Annotation, Mapping, Expression and Network

836   (AMEN) suite of tools for molecular systems biology. *BMC Bioinformatics* **9**, 86

837   (2008) PMID:18254954

838   76. Best D, Sahlender DA, Walther N, Peden AA & Adams IR. Sdmg1 is a

839   conserved transmembrane protein associated with germ cell sex determination

840   and germline-soma interactions in mice. *Development* **135**, 1415-1425 (2008)

841   PMID:18321981

842 **FIGURE LEGENDS**

843 **Figure 1. Ablation of *Nr5a1* is efficient from E13.5 onwards. (A-F)** Detection of

844 NR5A1 (red nuclear signals), YFP (green cytoplasmic signal), and HSD3B1 (red

845 cytoplasmic signal) by IHC on transverse histological sections of the testis of a

846 control (A,C,E) and a *Nr5a1*$^{SC-/-}$ mutant fetus (B,D,F) at E12.5 (A,B) and E13.5 (C-

847 F). Efficient excision of the reporter transgene by cre is assessed by YFP expression

848 in virtually all SC (arrows) as early as E12.5 (A,B). However, loss of NR5A1 in SC is

849 only achieved at E13.5 (compare C with D). At this stage, expression of NR5A1 is

850 maintained in Leydig cells (arrowheads in C,D), as identified on consecutive sections

851 by their expression of HSD3B1 (E,F). Nuclei are counterstained with DAPI (blue

852 signal). Scale bar (in F): 50 μm.

853 **Figure 2. Ablation of *Nr5a1* in Sertoli cells impairs AMH and SOX9 expression.**

854 **(A-R)** Detection of AMH, SOX9 and GATA4 (red signals) on transverse histological

855 sections of testes of control (A,C,E,G,I,K,M,O,Q) and *Nr5a1*$^{SC-/-}$ mutant fetuses

856 (B,D,F,H,J,L,N,P,R) at E12.5 (A,B,G,H,M,N), E13.5 (C,D,I,J,O,P) and E14.5

857 (E,F,K,L,Q,R). In (G-R) nuclei are counterstained with DAPI (blue signal). Insets (in

858 K,L) are high magnifications showing nuclear localisation of SOX9 in control SC

859 versus cytoplasmic localisation in mutant SC. Note that at each developmental stage,

860 AMH, SOX9 and GATA4 IHC are performed on consecutive sections. Scale bar (in

861 R): 50 μm. (**S**) RT-qPCR analyses comparing the expression levels of *Amh*, *Sox9*,

862 *Sox8* and *Ptgds* mRNAs in whole testis RNA from control (n=4) and *Nr5a1*$^{SC-/-}$

863 mutant (n=4) fetuses at E13.5 and E14.5. Each point represents the mean value of a

864 technical triplicate, and the bars indicate the mean value.

865 **Figure 3. NR5A1-deficient Sertoli cells die even when they lack TRP53. (A,D)**

866 Detection of YFP (green signal) and TUNEL-positive cells (red signal) on histological

867   sections from testis of control (A) and $Nr5a1^{SC-/-}$ mutant fetuses (B) at E14.5 (A,B)

868   and E15.5 (C,D). **(E,F)** Detection of GATA4 (red signal) and TUNEL-positive cells

869   (green signal) on histological sections of control (E) and $Nr5a1^{SC-/-}$ mutant testes (F)

870   fetuses at E14.5. Nuclei are counterstained with DAPI (blue signal). Arrowheads

871   point to TUNEL-positive SC in the mutant. **(G,H)** Detection of TRP53 (brown signal)

872   on histological sections of control (G) and $Nr5a1^{SC-/-}$ mutant (H) testes at E14.5. The

873   insets show larger magnifications. Arrowheads and arrows point to SC and GC,

874   respectively. **(I,J)** Detection of SOX9 (red signal) and YFP (green signal) by IHC on

875   histological sections of $Nr5a1^{SC-/-}$ (I) and $Nr5a1^{SC-/-};Trp53^{SC-/-}$ (J) mutants at E14.5.

876   Arrowheads point to SC. **(K-M)** Haematoxylin and eosin staining (H&E) on

877   histological sections of testes from control (K), $Nr5a1^{SC-/-}$ (L) and $Nr5a1^{SC-/-};Trp53^{SC-}$

878    $^{/-}$ (M) mutants at PND15. **(N-P)** Detection of HSB3B1 (red signal) on transverse

879   histological sections of testes from control (N), $Nr5a1^{SC-/-}$ (O) and $Nr5a1^{SC-/-}$

880    $;Trp53^{SC-/-}$ mutants (P) at PND15. **(Q-S)** Detection of HSB3B1 (red signal) on

881   transverse histological sections of testes from control (Q), $Nr5a1^{SC-/-}$ (R) and

882    $Nr5a1^{SC-/-};Trp53^{SC-/-}$ mutants (s) at PND60. The dotted white lines (in K,N,Q)

883   delineate seminiferous tubules. Nuclei are counterstained with DAPI (blue signal).

884   LC, Leydig cells. Scale bar (in S): 25 μm (A-D,I,J), 15 μm (E,F), 100 μm (G,H), 80 μm

885   (K-P), 20 μm (Q-S).

886   **Figure 4. Abnormal external genitalia and Müllerian duct retention in $Nr5a1^{SC-/-}$**

887   **males. (A,C)** Anogenital distance in control and $Nr5a1^{SC-/-}$ males at PND60. **(B,D)**

888   Penis bones dissected from control and $Nr5a1^{SC-/-}$ males at PND60 and stained with

889   alizarin red and alcian blue. **(E-H)** Reproductive tracts of control (E) and $Nr5a1^{SC-/-}$

890   (F-H) males at PN60. **(I-J)** Histological sections from the $Nr5a1^{SC-/-}$ mutant sample

891   shown in (H) and stained by H&E. The uterine surface consists of a simple columnar

892   epithelium and the vaginal epithelium is typically stratified squamous. Legend: A,

893   ampullary gland; CP, cranial prostate; E, epididymis; F, fat pad; SV, seminal vesicle;

894   T, testis; UB, uterus body; UH, uterine horn; V, vagina; VD, vas deferens; VP, ventral

895   prostate. Scale bar (in J): 10 μm (I,J).

896   **Figure 5. Transcriptomes of control and *Nr5a1*^{SC–/–} testicular cells at a single-**

897   **cell resolution. (A)** UMAP plot of single cell transcriptomes from control (blue) and

898   *Nr5a1*^{SC–/–} (pink) testes at E14.5, partitioned into 23 cell clusters (named C1-C23) by

899   using Seurat graph-based clustering. The proportion of control and mutant cells in

900   each cell cluster is indicated below as coloured bars. Legend: Legend: coel. ep.,

901   coelomic epithelium. **(B,C)** Volcano plots of differential gene expression in GC (panel

902   B, clusters C22 and C23) and SC (panel C, clusters C18, C19 and C21) from control

903   and *Nr5a1*^{SC–/–} testes. Red dots correspond to genes deregulated more than 1.2-fold.

904   **(D-K)** Detection of ALDH1A1, TMEM184A (red signals), TRA98, AMH, DDX4 (green

905   signals) or TUBB3 and PCP4 (brown signals) by IHC on transverse histological

906   sections of control (D-G) and *Nr5a1*^{SC–/–} mutant (H-K) testes at E14.5. In (D,E,H,I)

907   nuclei are counterstained with DAPI (blue signal). The dotted lines (in D,I) delimit

908   seminiferous cords. The arrowheads (in G,L) point to SC nuclei. Scale bar (in K):

909   25 μm (D,E,H,I), 100 μm (F,J), 15 μm (G,K). (**L**) RT-qPCR analyses comparing the

910   expression levels of selected mRNAs as indicated in whole testis RNA from control

911   (n=4) and *Nr5a1*^{SC–/–} mutant (n=4) fetuses at E14.5. Each point represents the mean

912   value of a technical triplicate, and the bars indicate the mean value.

913   **Figure 6. NR5A1-deficient Sertoli change their identity. (A)** Predicted projection of

914   control (blue) and *Nr5a1*^{SC–/–} (pink) cells on a reference single-cell transcriptomic

915   atlas of gonad development. **(B,C)** Dot plots representing the predicted association of

916   cell clusters from the control and *Nr5a1*^{SC–/–} single-cell dataset (y axis) to cell-types

917   (panel B) and to sex and developmental stages (panel C) according to the atlas

918   previously published [29] (x axis). The dot size represents the prediction score

919   (ranging from 0.0 to 1.0) of a given cell cluster to be associated with a given cell-type

920   based on the TransferData function implemented in Seurat. The color intensity (from

921   white to dark red) indicates the percentage of cells of a given cell cluster that have

922   been associated with a given cell-type. Legend: coel., coelomic; ctrl, control; ep.,

923   epithelium; mes., mesenchyme; meso., mesonephros; mut, mutant; prog., progenitor.

924   **(D,E)** Detection of FOXL2 (red signal) and DDX4 (green signal) by IHC on transverse

925   histological sections of control (D) and *Nr5a1*$^{SC-/-}$ mutant (G) testes at E15.5. Nuclei

926   are counterstained with DAPI (blue signal). The inset (in D) shows detection of

927   FOXL2 in a E15.5 fetal ovary, used as a positive control for IHC. Scale bar (in E):

928   15 µm (D,E).

929   **Figure 7. Loss of NR5A1 in Sertoli cells induces disorganisation of the testis**

930   **cords. (A,B,E,F)** Histological sections through E14.5 (A,E) and E15.5 (B,F) control

931   (A,B) and *Nr5a1*$^{SC-/-}$ mutant (E,F) fetuses stained by hematoxylin and eosin (H&E).

932   In controls, the seminiferous cords are well defined (dotted lines). In mutants, they

933   are poorly defined from E14.5 onwards (broken dotted lines with arrows). **(C,D,G,H)**

934   Detection of COL-IV, SOX9 (red signals), and YFP (green signal) on transverse

935   histological sections of the testis from control (C,D) and *Nr5a1*$^{SC-/-}$ mutant fetuses

936   (G,H) at E14.5. Note that (C,D) and (G,H) are consecutive sections. Arrows (in G)

937   point to the loss of COL-IV at the periphery of seminiferous cords, where SOX9 is lost

938   in SC (arrowheads in H). Scale bar (in D): 10 µm (A,B,E,F), 15 µm (C,D,G,H). **(I)**

939   Tukey box plots illustrating medians, ranges and variabilities of log normalized

940   expression of the indicated genes involved in either cell junction/adhesion (CJA) or

941   ECM composition.

942   **Figure 8. Summary of the alterations induced by the loss of NR5A1 in Sertoli**

943   **cells after the sex determination period. (A)** Control situation. **(B)** *Nr5a1*$^{SC-/-}$

944   mutant situation. Blue and yellow ovals are up- and down-regulated genes,

945   respectively. Legend: AGD, anogenital distance; PGD2, prostaglandin D2.

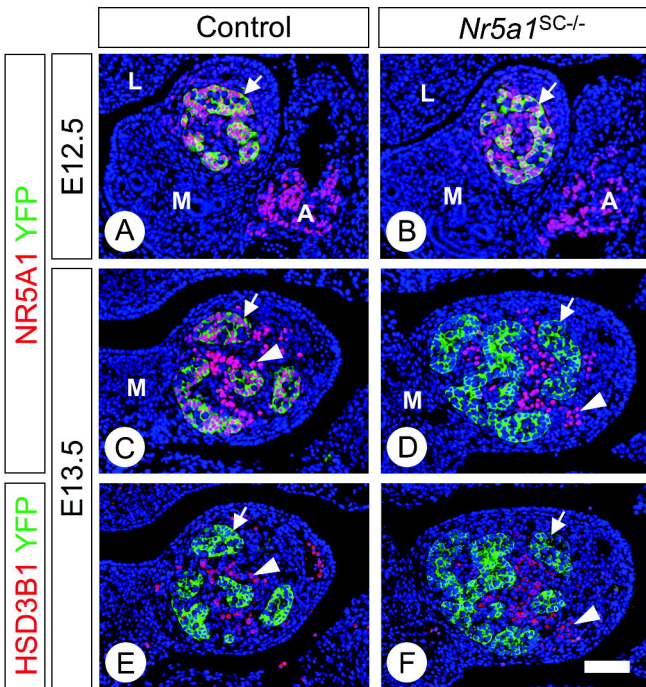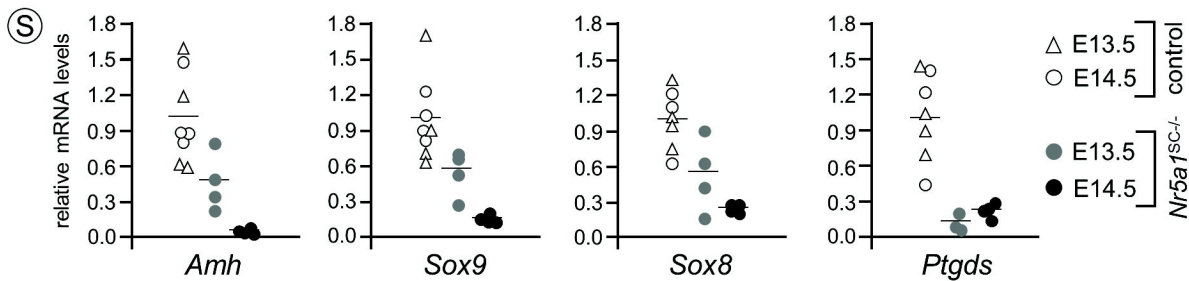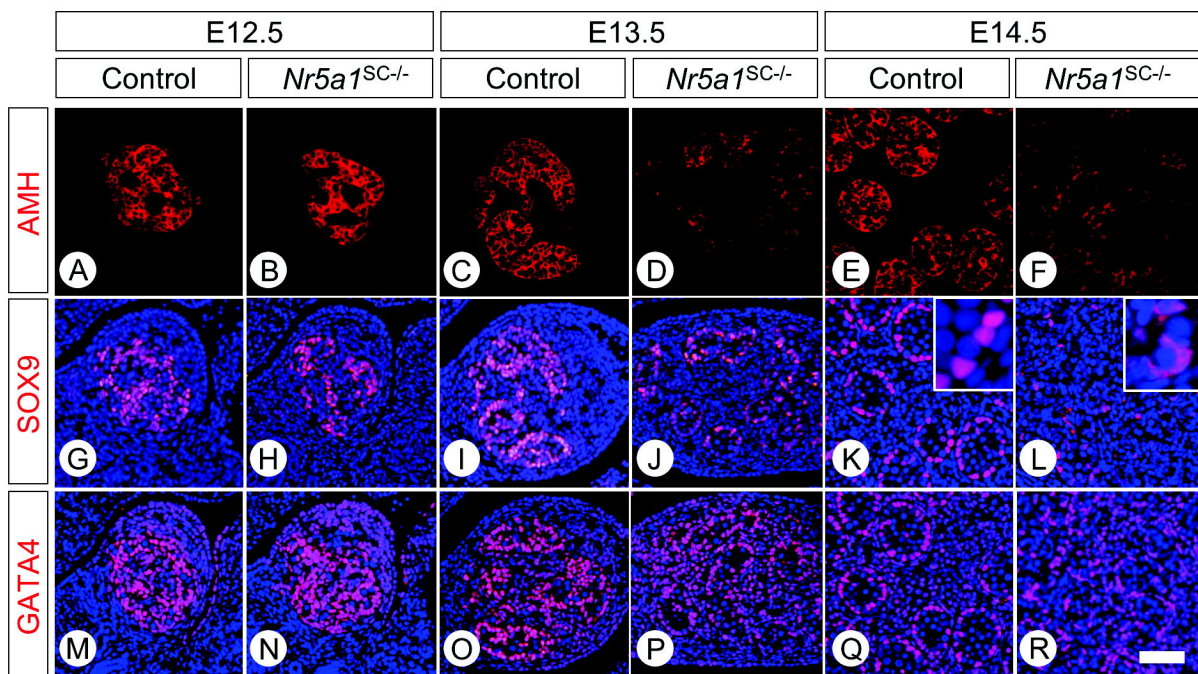**Table 1.** Primary antibodies used for immunohistochemistry experiments.

Antibodies	Species	Dilution	Source	Reference
ALDH1A1	Rabbit polyclonal	1/50	Abcam	ab52492
ALDH1A3	Rabbit polyclonal	1/20	Sigma	HPA046271C106318
AMH	Goat polyclonal	1/100	Santa-Cruz	sc-6886
BHMT	Rabbit polyclonal	1/200	Anticorps-enligne.fr	ABIN310161
BrdU	Rat monoclonal	1/100	Bio Rad	OBT0030S
COL-IV	Rabbit polyclonal	1/50	Abcam	ab19808
DDX4	Rabbit polyclonal	1/2000	Abcam	ab13840
FOXL2	Goat polyclonal	1/250	Abcam	ab5096
GATA 4	Goat polyclonal	1/50	Santa-Cruz	sc-1237
H2AFX	Mouse monoclonal	1/500	Millipore	05-636 (JBW301)
HSD3B1	Rabbit polyclonal	1/1000	Trans Genic's Inc	KO607
NR5A1	Rabbit polyclonal	1/100	Cosmo Bio	KAL-KO611
PAX8	Mouse monoclonal	1/10	Abcam	ab53490
PCP4	Rabbit polyclonal	1/500	Novus Biologicals	NBP1-80929
REC8	Rabbit monoclonal	1/200	Abcam	ab192241
SOX8	Mouse monoclonal	1/100	Novus Biologicals	H00030812-M01
SOX9	Rabbit polyclonal	1/1000	Sigma Aldrich	ab5535
SOX10	Goat polyclonal	1/1000	R&D Systems	AF2864
STRA8	Rabbit polyclonal	1/1000	Abcam	ab49602
TMEM184A	Rabbit polyclonal	1/200		[76]
TRA98	Rat monoclonal	1/500	Abcam	ab82527
TRP53	Rabbit polyclonal	1/200	Santa-Cruz	sc-6243
TUBB3	Mouse monoclonal	1/1000	Covance	MMS-435P-0100 (TUJ1 clone)
WT1	Mouse monoclonal	1/500	Cell Marque	348M-94
YFP	Chicken polyclonal	1/500	Aves	GFP-1020

Table 2. Primers used for quantification of mRNA levels by real-time RT-qPCR.
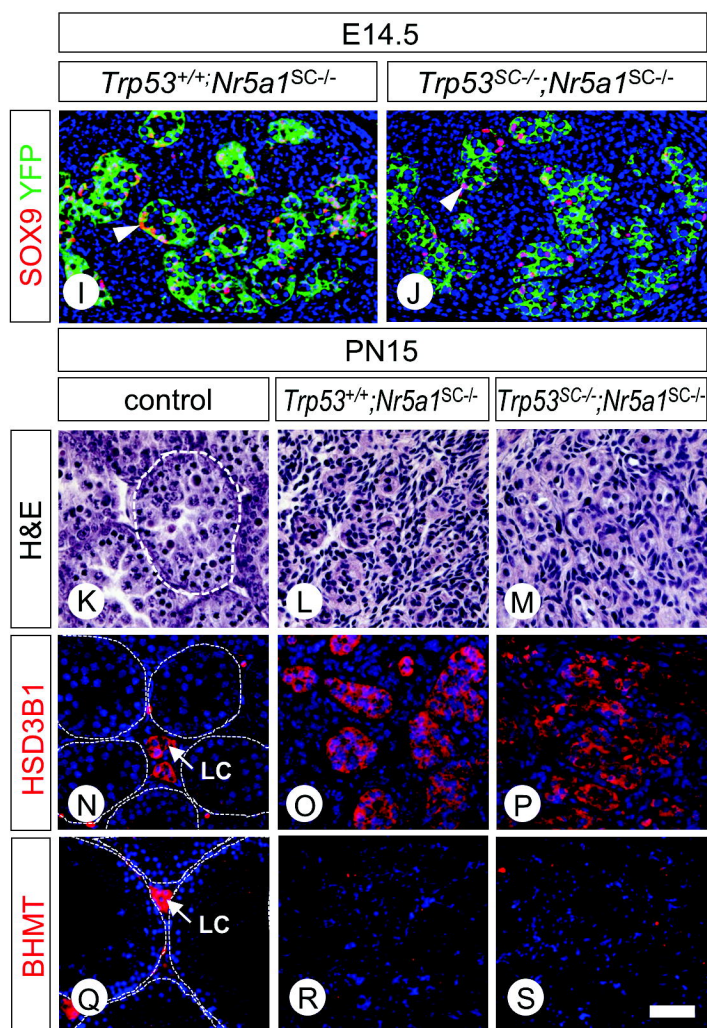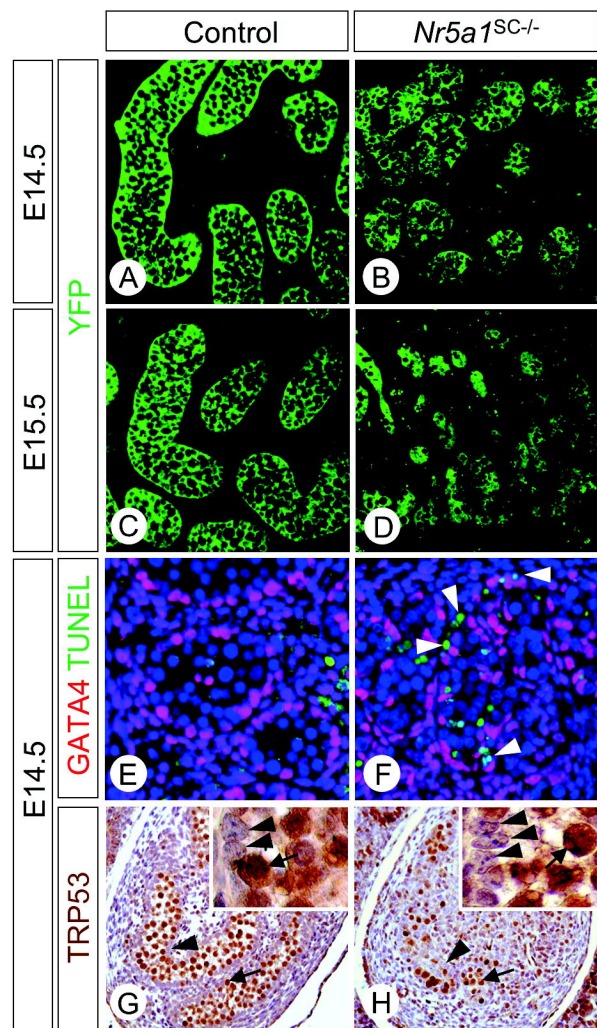

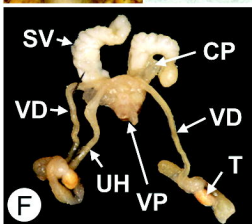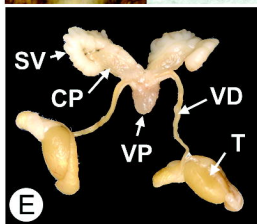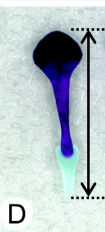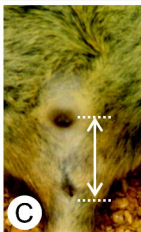| Gene	Accession number	Forward primer sequence	Reverse primer sequence	Amplicon size (bp)
Amh	NM_007445.3	5'-TCCTACATCTGGCTGAAGTGATATG-3'	5'-CAGGTGGAGGCTCTTGGAACT-3'	66
Col6a6	NM_001102607.1	5'-TGATTGCGTTCAGCAACGTG-3'	5'-TCCGGCTTGCATAGATCATAG-3'	157
Cyp26b1	NM_001177713.1	5'-CGACATCCACCGCAACAAG-3'	5'-GGCCTCCTGATATACATTGATGG-3'	151
Dhh	NM_007857.5	5'-GCACAGGATTCACTCCACTACGA-3'	5'-CCAGTGAGTTATCAGCTTTGACC-3'	172
Fst	NM_001301373.1	5'-CTGCTGCTACTCTGCCAGTT-3'	5'-ACATCCTCCTCGGTCCATGA-3'	167
Hsd17b3	NM_008291.3	5'-ATGGAGTCAAGGAGGAAAGGC-3'	5'-ATGGAGTCAAGGAGGAAAGGC-3'	76
Inhbb	NM_008381.4	5'-GCGTCTCCGAGATCATCAGC-3'	5'-CACCTTGACCCGTACCTTCC-3'	188
Itga6	NM_001277970.1	5'-GCGGCTACTTTCACTAAGGACT-3'	5'-TTCTTTTGTTCTACACGGACGA-3'	92
Pcp4	NM_008791.3	5'-GCGACCAACGGAAAAGACAA-3'	5'-TTCAGGTGGACCAGGAAGCA-3'	194
Ptgds	NM_008963.3	5'-GCTCTTCGCATGCTGTGGAT-3'	5'-GCCCCAGGAACTTGTCTTGTT-3'	118
Sox8	NM_011447.3	5'-ACCCGCATCTCCATAACGCA-3'	5'-TGGTGGCCCAGTTCAGTACC-3'	214
Sox9	NM_011448.4	5'-CAGCAAGACTCTGGGCAAG-3'	5'-TCCACGAAGGGTCTCTTCTC-3'	63
Tubb3	NM_023279.3	5'-CGTGAAGTCAGCATGAGGGA-3'	5'-TCCAAGTCCACCAGAATGGC-3'	218

	Control	*Nr5a1*$^{SC-/-}$

	E12.5		E13.5		E14.5	
	Control	$Nr5a1^{SC-/-}$	Control	$Nr5a1^{SC-/-}$	Control	$Nr5a1^{SC-/-}$
AMH	A	B	C	D	E	F
SOX9	G	H	I	J	K	L
GATA4	M	N	O	P	Q	R

S — relative mRNA levels

Amh *Sox9* *Sox8* *Ptgds*

△ E13.5] control
○ E14.5]

● E13.5] $Nr5a1^{SC-/-}$
● E14.5]

Control $Nr5a1^{SC-/-}$

A   B   C   D

SV   CP   SV   CP
    VD   VD   VD
    VP   UH VP
        T   T
E   F

$Nr5a1^{SC-/-}$

    E F   UH   UB   UH
E   T   V
F   U   U   A   Ur
    VD   VD
G   H

I   J

A

control   *Nr5a1*^SC-/-

Sertoli
C18
immune
C2
Leydig
C5
C4
erythrocyte
C1
C17
perivascular
C8
C13   **C9**
C15   C7   C6
C14   C11   C10
C19
coel.ep.
C12
C20
rete
C16   interstitial
germ
C21
C3   C22   C23
mutant Sertoli   endothelial

Frequency

C1 C2 C3 C4 C5 C6 C7 C8 C9 C10 C11 C12 C13 C14 C15 C16 C17 C18 C19 C20 C21 C22 C23

100 75 50 25 0

erythrocyte immune endothelial Leydig interstitial coel. ep. perivascular **Sertoli rete mutant Sertoli** germ

B

-log10(p-value)

120 90 60 30 0

Stra8
Gdpd3
Id1
Nanos2   *Smc1b*
Rec8
Piwil4
germ cells

-2   -1   0   1   2
Log2 fold-change

C

-log10(p-value)

300 200 100 0

Aldh1a1
Hsd17b3   *Col6a6*
Amh
Tmem184a   *Fst*
Ptgds   *Rspo1*
Itga6   *Pcp4*
Sox9
Wnt4
Cyp26b1
Tubb3
Sertoli cells

-2.5   0   2.5
Log2 fold-change

E14.5

ALDH1A1 TRA98 | TMEM184A AMH | TUBB3 | PCP4

Control

Nr5a1^SC-/-

L

relative mRNA levels

2.5 2.0 1.5 1.0 0.5 0.0

Cyp26b1   *Dhh*   *Hsd17b3*   *Inhbb*   *Itga6*

control   *Nr5a1*^SC-/-

relative mRNA levels

10 8 6 4 2 0

Fst   *Col6a6*   *Pcp4*

Figure panels labeled:

E14.5 — E15.5 — E14.5

H&E — H&E — COL-IV YFP — SOX9 YFP

Control | A B C D

$Nr5a1^{SC-/-}$ | E F G H

(I) Log normalized counts

control | $Nr5a1^{SC-/-}$

Gja1 — Jam2 — Itga6 — Ptk2b | Mdk — Fn1 — Fbln1 — Mgp — Col4a1 — Col4a2 — Col3a1 — Col5a2 — Col6a6

CJA | ECM

A control situation

anchoring → survival structured cord

basement membrane

germ cell

Nanos2

Stra8

Meiosis

Rec8 *Sycp3*

Sertoli cell

Wnt4 *Rspo1*

PGD2

Ptgds

Nr5a1

Sox9 *Sox8*

Col4a1 *Col4a2* *Itga6*

Dhh

Cyp26b1

Amh

Hsd17b1 *Hsd17b3*

Leydig cell

Ptch1

Hsd3b1

androstene-dione

Müllerian (regression)

Testosterone → AGD, penis

B *Nr5a1*^SC-/- situation

detachment → death cord structure lost

basement membrane

germ cell

Nanos2

Stra8

Meiosis

Rec8 *Sycp3*

Sertoli cell

Wnt4 *Rspo1*

PGD2

Ptgds

Nr5a1 ✕

Sox9 *Sox8*

Col4a1 *Col4a2* *Itga6*

Dhh

Cyp26b1

Amh

Hsd17b1 *Hsd17b3*

Leydig cell

Ptch1

Hsd3b1

androstene-dione

Müllerian (persistence)

Testosterone → AGD, penis